

## Full length article

# Thermal and mechanical stability of functionally graded carbon nanotubes (FG CNT)-reinforced composite truncated conical shells surrounded by the elastic foundations



Nguyen Dinh Duc<sup>a,\*</sup>, Pham Hong Cong<sup>a,b</sup>, Ngo Duc Tuan<sup>c</sup>, Phuong Tran<sup>c</sup>, Nguyen Van Thanh<sup>d</sup>

<sup>a</sup> Advanced Materials and Structures Laboratory, VNU-Hanoi, University of Engineering and Technology, 144 Xuan Thuy, Cau Giay, Hanoi, Vietnam

<sup>b</sup> Centre for Informatics and Computing (CIC), Vietnam Academy of Science and Technology, 18 Hoang Quoc Viet - Cau Giay, Hanoi, Vietnam

<sup>c</sup> Department of Infrastructure Engineering, The University of Melbourne, Parkville 3010, VIC, Australia

<sup>d</sup> Military Academy of Logistics, Ngoc Thuy, Long Bien, Hanoi, Vietnam

## ARTICLE INFO

## Keywords:

Thermal and mechanical stability  
Functionally graded carbon nanotube fibers-reinforced composite (FG CNTRC) truncated conical shell  
Elastic foundations

## ABSTRACT

The thermal and mechanical stability of a functionally graded composite truncated conical shell reinforced by carbon nanotube fibers and surrounded by the elastic foundations are studied in this paper. Distribution of reinforcements across the shell thickness is assumed to be uniform or functionally graded. The equilibrium and linearized stability equations for the shells are derived based on the classical shell theory. Using Galerkin method, the closed – form expression for determining the linear thermal and mechanical buckling load is obtained. The paper also analyzed and discussed the effects of semi-vertex angle, shell length, volume fraction of fibers, distribution pattern of fibers, temperature, elastic foundations on the linear thermal and mechanical buckling loads of the functionally graded carbon nanotube fibers-reinforced composite (FG CNTRC) truncated conical shell in thermal environment.

## 1. Introduction

Carbon nanotubes (CNTs) have attracted increasing attention in recent years due to their exceptional thermal, mechanical and electrical properties. For example, their Young's moduli are superior to all carbon fibers with a value greater than 1 TPa and their density can be only 1.3 g/cm<sup>3</sup> [1]. Due to such interesting features, CNTs are selected as a promising candidate to reinforce the composites [1]. Functionally graded materials (FGM), which are microscopic composites made from a mixture of metal and ceramic constituents, were first introduced in 1984 by a group of Japanese materials scientists [2], recently, these studies have mainly focused on the nonlinear static and dynamic stability analysis of FGM plates and shells [3]. Functionally graded materials involving conical shells are widely used in exhaust nozzles of solid rocket engines, space vehicles, aircrafts, nuclear power plants and many other engineering applications. Unique features of FGM and CNTs may be achieved together, for instance, through functionally graded distributions of CNTs in a FGM media. Functionally graded carbon nanotube-reinforced composites (FG CNTRC) were first introduced by Shen [4].

The static stability and dynamic of plates and shells reinforced by CNTs fibers has been studied by many researchers in recent years. Jafari

et al. [5] studied the mechanical buckling of nano-composite rectangular plate reinforced by aligned and straight single walled carbon nanotubes. Lei et al. [6] presented the buckling analysis of FG CNTRC plates using the element-free kp-Ritz method. Jam and Kiani [7] investigated the buckling of pressurized FG CNTRC conical shells using the first order shear deformation shell theory but did not study thermal instability. Jalali and Heshmati [8] studied the buckling analysis of circular sandwich plates with tapered cores and functionally graded carbon nanotubes-reinforced composite face sheets. Zhang et al. [9] investigated the vibration analysis of functionally graded carbon nanotube reinforced composite thick plates with elastically restrained edges. Ansari and Torabi [10] studied the buckling and vibration of functionally graded carbon nanotube-reinforced composite conical shells under axial loading.

In fact, the structures are often put under the environment with high temperatures. Zhang et al. [11] studied the postbuckling of CNTRC cylindrical shells in thermal environments. Shen [12–14] investigated the postbuckling of CNTRC cylindrical shells in thermal environments with axially-loaded shells [12] and pressure-loaded shells [13], torsional postbuckling [14] and under combined axial and radial mechanical loads [15]. Shen and Zhu [16] investigated the buckling and postbuckling behavior of FG CNTRC plates in thermal

\* Corresponding author.

E-mail address: [ducnd@vnu.edu.vn](mailto:ducnd@vnu.edu.vn) (N.D. Duc).

environments. Torabi et al. [17] studied the linear thermal buckling analysis of truncated hybrid FGM conical shells. Akbari et al. [18] considered the thermal buckling of temperature dependent FGM conical shells with arbitrary edge supports. Sofiyev et al. [19] presented the thermoelastic buckling of FGM conical shells under non-linear temperature rise in the framework of the shear deformation theory. Shen and Zhang [20] studied the thermal buckling and postbuckling behavior of FG CNTRC plates. Naj et al. [21] investigated the thermal and mechanical instability of FGM graded truncated conical shells. Mirzaei and Kiani [22] considered the thermal buckling of temperature dependent FG CNTRC conical shells. Duc et al. [23,24] studied the mechanical and thermal stability of eccentrically stiffened FGM conical shell surrounded by the elastic foundations and in thermal environment.

These researches about plates and shells made by CNTRC surrounded by the elastic foundations are also studied. Shen and Xiang investigated the postbuckling of axially compressed CNTRC cylindrical panels [25] and the nonlinear analysis of CNTRC beams [26] resting surrounded by an elastic foundation in thermal environments. Zhang et al. [27] used the element-free IMLS-Ritz framework for buckling analysis of FG CNTRC thick plates resting on Winkler foundation. Lei et al. [28] considered the buckling of FG CNTRC thick skew plates resting on Pasternak foundation based on an element-free approach. Shen and Xiang studied the thermal postbuckling of CNTRC cylindrical shells [29] and FG CNTRC cylindrical panels resting surrounded by an elastic foundation [30].

From above studies, it can be seen that there has not got any research studying about the mechanical and thermal buckling analysis of FG CNTRC truncated conical shells.

This paper studies the linear thermal and mechanical instability of the FG CNTRC truncated conical shells reinforced by CNTs fibers and surrounded by the elastic foundations in thermal environment. The equilibrium and linearized stability equations for the shells are derived based on the classical shell theory. Using Galerkin method, the closed – form expression for determining the thermal and mechanical buckling load is obtained. The material properties were assumed to be temperature-dependent leading to the equation to determine buckling thermal loads with both sides that are dependent on temperature, so the iterative algorithms are proposed to solve this problem. The paper also analyzes and discusses the effects of semi-vertex angle, shell length, volume fraction of fibers, distribution pattern of fibers, temperature, elastic foundations on the linear thermal and mechanical buckling loads of the FG CNTRC truncated conical shell.

## 2. FG CNTRC truncated conical shells surrounded by the elastic foundations

Consider a FG CNTRC truncated conical shells and surrounded by the elastic foundations, conical shell of thickness  $h$ , and radii  $R_1 < R_2$ , length  $L$  and vertex half angle  $\alpha$ . The meridional, circumferential, and normal directions of the shell are denoted by  $x$ ,  $\theta$  and  $z$ , respectively. A schematic of the shell with the assigned coordinate system and geometric characteristics are shown in Fig. 1.

The single walled carbon nanotube (SWCNT) reinforcement is either uniformly distributed or functionally graded in the thickness direction [4–9]. FG-V and FG- $\Lambda$  CNTRC (Fig. 2) are the functionally graded distraction of CNTs through the thickness direction of the composite truncated conical shell.

The effective material properties may be written as [4–9]:

$$\begin{aligned} E_{11} &= n_1 V_{CN} E_{11}^{CN} + V_m E^m \\ \frac{n_2}{E_{22}} &= \frac{V_{CN}}{E_{22}^{CN}} + \frac{V_m}{E^m} \\ \frac{n_3}{G_{12}} &= \frac{V_{CN}}{G_{12}^{CN}} + \frac{V_m}{G^m} \end{aligned} \tag{1}$$

where in the above equations,  $E_{11}^{CN}$ ,  $E_{22}^{CN}$  and  $G_{12}^{CN}$  are Young's modulus and shear modulus of SWCNT, respectively. Besides,  $E^m$  and  $G^m$  indicate the corresponding properties of the matrix. The coefficients  $\eta_1$ ,  $\eta_2$ ,  $\eta_3$  are introduced to account for the scale dependent material properties. These constants are evaluated by matching the effective properties of CNTRC obtained from the MD simulations with those from the rule of mixtures. Furthermore, in Eq. (1),  $V_{CN}$  and  $V_m$  are the volume fractions of CNTs and matrix phase, respectively, which satisfy the condition

$$V_{CN} + V_m = 1 \tag{2}$$

Uniform and four types of functionally graded distributions of the CNTs along the thickness direction of the FG CNTRC conical shell are assumed. Mathematical expression of CNTs volume fraction in each case of distribution is given in Table 1.

The effective Poisson ratio depends weakly on position [4–9] and is expressed as

$$\nu_{12} = V_{CN}^* \nu_{12}^{CN} + V_m \nu^m \tag{3}$$

The thermal expansion coefficients in the longitudinal and transverse directions can be expressed by the Shapery model [15,16,21] as

$$\begin{aligned} \alpha_{11} &= \frac{V_{CN} E_{11}^{CN} \alpha_{11}^{CN} + V_m E^m \alpha^m}{V_{CN} E_{11}^{CN} + V_m E^m} \\ \alpha_{22} &= (1 + \nu_{12}^{CN}) V_{CN} \alpha_{22}^{CN} + (1 + \nu^m) V_m \alpha^m - \nu_{12} \alpha_{11} \end{aligned} \tag{4}$$

where in the above equations,  $\alpha_{11}^{CN}$ ,  $\alpha_{22}^{CN}$ ,  $\alpha^m$  are the thermal expansion coefficients of the constituents.

## 3. Basic formulation

The present study uses the classical shell theory with the geometrical nonlinearity in von Karman sense to establish the governing equations. Thus, the normal and shear strains at distance  $z$  from the middle surface of shell are [31,32]:

$$\epsilon_x = \epsilon_x^0 + z k_x, \quad \epsilon_\theta = \epsilon_\theta^0 + z k_\theta, \quad \gamma_{x\theta} = \gamma_{x\theta}^0 + 2z k_{x\theta}, \tag{5}$$

in which  $\epsilon_x^0$  and  $\epsilon_\theta^0$  are the normal strains and  $\gamma_{x\theta}^0$  is the shear strain at the middle surface of the shell, and  $k_x$ ,  $k_\theta$  and  $k_{x\theta}$  are the change of curvatures and twist, respectively. They are related to the displacement components as

$$\begin{aligned} \epsilon_x^0 &= \frac{\partial u}{\partial x} + \frac{1}{2} \left( \frac{\partial w}{\partial x} \right)^2, \\ \epsilon_\theta^0 &= \frac{1}{x \sin \alpha} \frac{\partial v}{\partial \theta} + \frac{u}{x} + \frac{w}{x} \cot \alpha + \frac{1}{2x^2 \sin^2 \alpha} \left( \frac{\partial w}{\partial \theta} \right)^2, \\ \gamma_{x\theta}^0 &= \frac{1}{x \sin \alpha} \frac{\partial u}{\partial \theta} - \frac{v}{x} + \frac{\partial v}{\partial x} + \frac{1}{x \sin \alpha} \frac{\partial w}{\partial x} \frac{\partial w}{\partial \theta}, \\ k_x &= -\frac{\partial^2 w}{\partial x^2}, \quad k_\theta = -\frac{1}{x^2 \sin^2 \alpha} \frac{\partial^2 w}{\partial \theta^2} - \frac{1}{x} \frac{\partial w}{\partial x}, \\ k_{x\theta} &= -\frac{1}{x \sin \alpha} \frac{\partial^2 w}{\partial x \partial \theta} + \frac{1}{x^2 \sin \alpha} \frac{\partial w}{\partial \theta}. \end{aligned} \tag{6}$$

Hooke law for the FG CNTRC shells using the classical shell theory can be defined as [31,32]:

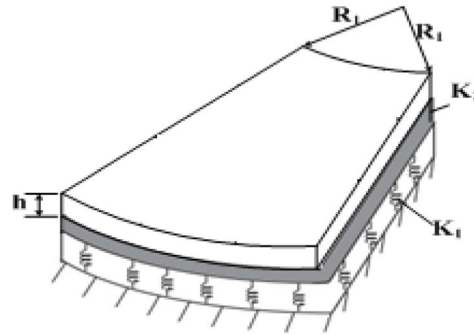
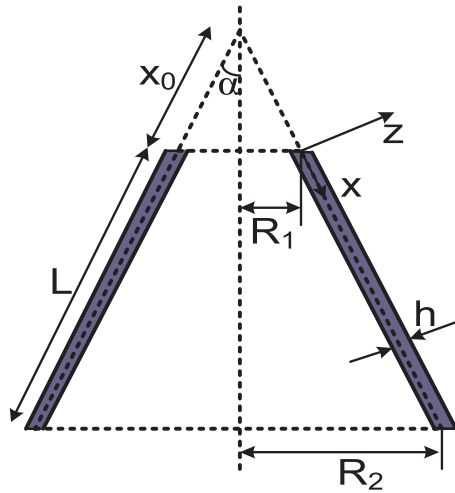


Fig. 1. The geometry of a FG CNTRC truncated conical shell surrounded by the elastic foundations.

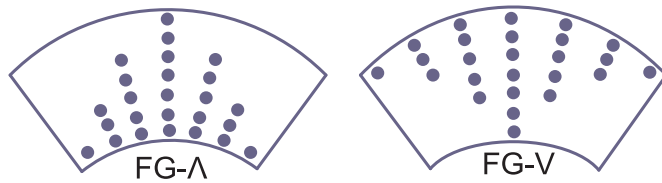


Fig. 2. Configurations of various CNTRC truncated conical shells.

Table 1  
Volume fraction of CNTs as a function of thickness coordinate for various cases of CNTs distribution [4–9].

CNTs distribution	$V_{CN}$
FG-V CNTRC	$V_{CN}^* \left(1 + 2\frac{z}{h}\right)$
FG-Λ CNTRC	$V_{CN}^* \left(1 - 2\frac{z}{h}\right)$

$$\begin{Bmatrix} \sigma_{xx} \\ \sigma_{\theta\theta} \\ \sigma_{x\theta} \end{Bmatrix} = \begin{bmatrix} Q_{11} & Q_{12} & 0 \\ Q_{12} & Q_{22} & 0 \\ 0 & 0 & Q_{44} \end{bmatrix} \begin{Bmatrix} \epsilon_x - \alpha_{11}\Delta T \\ \epsilon_\theta - \alpha_{22}\Delta T \\ \gamma_{x\theta} \end{Bmatrix} \quad (7)$$

where  $\Delta T$  is temperature rise from stress free initial state or temperature difference between two surfaces of the shell. Beside,  $Q_{ij}$  are the reduced material stiffness coefficients compatible with plane-stress conditions and are obtained as follow

$$Q_{11} = \frac{E_{11}}{1 - \nu_{12}\nu_{21}}, \quad Q_{22} = \frac{E_{22}}{1 - \nu_{12}\nu_{21}}, \quad Q_{12} = \frac{\nu_{21}E_{11}}{1 - \nu_{12}\nu_{21}}, \quad Q_{44} = G_{23} \quad (8)$$

Integrating the above stress–strain equations and their moments through the thickness of the shell, we obtain the expressions for force and moment resultants as

$$\begin{aligned} N_x &= A_{11}\epsilon_x^0 + A_{12}\epsilon_\theta^0 + B_{11}k_x + B_{12}k_\theta - N_{xx}^T, \\ N_\theta &= A_{12}\epsilon_x^0 + A_{22}\epsilon_\theta^0 + B_{12}k_x + B_{22}k_\theta - N_{\theta\theta}^T, \\ N_{x\theta} &= A_{66}\gamma_{x\theta}^0 + 2B_{66}k_{x\theta}, \\ M_x &= B_{11}\epsilon_x^0 + B_{12}\epsilon_\theta^0 + D_{11}k_x + D_{12}k_\theta - M_{xx}^T, \\ M_\theta &= B_{12}\epsilon_x^0 + B_{22}\epsilon_\theta^0 + D_{12}k_x + D_{22}k_\theta - M_{\theta\theta}^T, \\ M_{x\theta} &= B_{66}\gamma_{x\theta}^0 + 2D_{66}k_{x\theta}, \end{aligned} \quad (9)$$

In the above equations, the constant coefficients  $A_{ij}$ ,  $B_{ij}$ ,  $D_{ij}$  ( $i = 1 \div 2, 6; j = 1 \div 2, 6$ ) indicate the stretching, bending–stretching, and bending stiffness, respectively, which are calculated by

$$\begin{Bmatrix} A_{ij} \\ B_{ij} \\ D_{ij} \end{Bmatrix} = \int_{-h/2}^{h/2} \begin{Bmatrix} Q_{ij} \\ zQ_{ij} \\ z^2Q_{ij} \end{Bmatrix} dz \quad (10)$$

Also,  $N_{ii}^T$ ,  $M_{ii}^T$  are included thermal force and moment resultants which may be calculated upon integrations as

$$\begin{bmatrix} N_{xx}^T & M_{xx}^T \\ N_{\theta\theta}^T & M_{\theta\theta}^T \end{bmatrix} = \int_{-h/2}^{h/2} \begin{bmatrix} Q_{11} & Q_{12} \\ Q_{12} & Q_{22} \end{bmatrix} \begin{bmatrix} \alpha_{11} \\ \alpha_{22} \end{bmatrix} (T - T_0) dz \quad (11)$$

The nonlinear equilibrium equations of the truncated conical shells surrounded by the elastic foundations based on the classical shell theory are given by [23,24,31]:

$$x \frac{\partial N_x}{\partial x} + \frac{1}{\sin \alpha} \frac{\partial N_{x\theta}}{\partial \theta} + N_x - N_\theta = 0, \quad (12a)$$

$$\frac{1}{\sin \alpha} \frac{\partial N_\theta}{\partial \theta} + x \frac{\partial N_{x\theta}}{\partial x} + 2N_{x\theta} = 0, \quad (12b)$$

$$\begin{aligned} &x \frac{\partial^2 M_x}{\partial x^2} + 2 \frac{\partial M_x}{\partial x} + \frac{2}{\sin \alpha} \left( \frac{\partial^2 M_{x\theta}}{\partial x \partial \theta} + \frac{1}{x} \frac{\partial M_{x\theta}}{\partial \theta} \right) \\ &+ \frac{1}{x \sin^2 \alpha} \frac{\partial^2 M_\theta}{\partial \theta^2} - \frac{\partial M_\theta}{\partial x} - N_\theta \cot \alpha + \left( x N_x \frac{\partial w}{\partial x} + \frac{1}{\sin \alpha} N_{x\theta} \frac{\partial w}{\partial \theta} \right)_{,x} \\ &+ \frac{1}{\sin \alpha} \left( N_{x\theta} \frac{\partial w}{\partial x} + \frac{1}{x \sin \alpha} N_\theta \frac{\partial w}{\partial \theta} \right)_{,\theta} - x K_1 w + x K_2 \nabla^2 w = 0, \end{aligned} \quad (12c)$$

where  $K_1$  ( $N/m^3$ ) is the Winkler foundation stiffness, and  $K_2$  ( $N/m$ ) is the shear subgrade modulus of the Pasternak foundation model.

The stability equations of conical shell are derived using the adjacent equilibrium criterion in Brush and Almroth [32], Naj et al. [21]. Assume that the equilibrium state of FG CNTRC conical shell under thermal loads is defined in terms of the displacement components  $u_0$ ,  $v_0$  and  $w_0$ . We give an arbitrarily small increments  $u_1$ ,  $v_1$  and  $w_1$  to the displacement variables, so the total displacement components of a neighboring state are:

$$u = u_0 + u_1, \quad v = v_0 + v_1, \quad w = w_0 + w_1. \quad (13)$$

Similarly, the force and moment resultants of a neighboring state

may be related to the state of equilibrium as:

$$\begin{aligned} N_x &= N_{x0} + N_{x1}, N_\theta = N_{\theta0} + N_{\theta1}, N_{x\theta} = N_{x\theta0} + N_{x\theta1}, \\ M_x &= M_{x0} + M_{x1}, M_\theta = M_{\theta0} + M_{\theta1}, M_{x\theta} = M_{x\theta0} + M_{x\theta1}, \end{aligned} \tag{14}$$

where terms with 0 subscripts correspond to the  $u_0, v_0, w_0$  displacements and those with 1 subscripts represents the portions of increments of force and moment resultants that are linear in  $u_1, v_1$  and  $w_1$ . The stability equations may be obtained by substituting Eqs. (13) and (14) into Eq. (12) and note that the terms in the resulting equations with subscript 0 satisfy the equilibrium equations and therefore drop out of the equations. In addition, the nonlinear terms with subscript 1 are ignored because they are small compared to the linear terms. The remaining terms form the stability equations as follows [10,19,23,31]:

$$x \frac{\partial N_{x1}}{\partial x} + \frac{1}{\sin \alpha} \frac{\partial N_{\theta1}}{\partial \theta} + N_{x1} - N_{\theta1} = 0, \tag{15a}$$

$$\frac{1}{\sin \alpha} \frac{\partial N_{\theta1}}{\partial \theta} + x \frac{\partial N_{x\theta1}}{\partial x} + 2N_{x\theta1} = 0, \tag{15b}$$

$$\begin{aligned} &x \frac{\partial^2 M_{x1}}{\partial x^2} + 2 \frac{\partial M_{x1}}{\partial x} + \frac{2}{\sin \alpha} \left( \frac{\partial^2 M_{x\theta1}}{\partial x \partial \theta} + \frac{1}{x} \frac{\partial M_{x\theta1}}{\partial \theta} \right) \\ &+ \frac{1}{x \sin^2 \alpha} \frac{\partial^2 M_{\theta1}}{\partial \theta^2} - \frac{\partial M_{\theta1}}{\partial x} - N_{\theta1} \cot \alpha \\ &+ \left( x N_{x0} \frac{\partial w_1}{\partial x} + \frac{1}{\sin \alpha} N_{x\theta0} \frac{\partial w_1}{\partial \theta} \right)_x + \frac{1}{\sin \alpha} \left( N_{x\theta0} \frac{\partial w_1}{\partial x} + \frac{1}{x \sin \alpha} N_{\theta0} \frac{\partial w_1}{\partial \theta} \right)_\theta \\ &- x K_1 w + x K_2 \nabla^2 w = 0. \end{aligned} \tag{15c}$$

Eq. (15a,b,c) are the stability equations of the FG CNTRC truncated conical shells. In Eq. (15a,b,c) the subscript 0 refers to the equilibrium state and subscript 1 refers to the stability state. The terms with the subscript 0 are the solution of the equilibrium equations for the given load.

Where the force and moment resultants for the state of stability are given by Naj et al. [21]:

$$\begin{aligned} N_{x1} &= A_{11} \epsilon_{x1}^0 + A_{12} \epsilon_{\theta1}^0 + B_{11} k_{x1} + B_{12} k_{\theta1}, \\ N_{\theta1} &= A_{12} \epsilon_{x1}^0 + A_{22} \epsilon_{\theta1}^0 + B_{12} k_{x1} + B_{22} k_{\theta1}, \\ N_{x\theta1} &= A_{66} \gamma_{x\theta1}^0 + 2B_{66} k_{x\theta1}, \\ M_{x1} &= B_{11} \epsilon_{x1}^0 + B_{12} \epsilon_{\theta1}^0 + D_{11} k_{x1} + D_{12} k_{\theta1}, \\ M_{\theta1} &= B_{12} \epsilon_{x1}^0 + B_{22} \epsilon_{\theta1}^0 + D_{12} k_{x1} + D_{22} k_{\theta1}, \\ M_{x\theta1} &= B_{66} \gamma_{x\theta1}^0 + 2D_{66} k_{x\theta1}, \end{aligned} \tag{16}$$

The linear form of the strains and curvatures in terms of the displacement components are:

$$\begin{aligned} \epsilon_{x1}^0 &= \frac{\partial u_1}{\partial x}, \\ \epsilon_{\theta1}^0 &= \frac{1}{x \sin \alpha} \frac{\partial v_1}{\partial \theta} + \frac{u_1}{x} + \frac{w_1}{x} \cot \alpha, \\ \gamma_{x\theta1}^0 &= \frac{\partial v_1}{\partial x} - \frac{v_1}{x} + \frac{1}{x \sin \alpha} \frac{\partial u_1}{\partial \theta}, \\ k_{x1} &= - \frac{\partial^2 w_1}{\partial x^2}, k_{\theta1} = - \frac{1}{x^2 \sin^2 \alpha} \frac{\partial^2 w_1}{\partial \theta^2} - \frac{1}{x} \frac{\partial w_1}{\partial x}, \\ k_{x\theta1} &= - \frac{1}{x \sin \alpha} \frac{\partial^2 w_1}{\partial x \partial \theta} + \frac{1}{x^2 \sin \alpha} \frac{\partial w_1}{\partial \theta}. \end{aligned} \tag{17}$$

### 3.1. Mechanical buckling

For simplicity, the membrane solution of the equilibrium equations

is considered (Naj et al. [21]). For this aim, all the moment and rotation terms must be set equal to zero in the equilibrium equations. By solving the membrane form of equilibrium equations, it is found that

$$N_{x0} = - \frac{P}{\pi x \sin 2\alpha}, N_{\theta0} = 0, N_{x\theta0} = 0 \tag{18}$$

where  $P$  is hydrostatic pressure.

Substituting Eqs. (16)–(17) into Eq. (15a,b,c), the stability equations in terms of the displacement component are of the forms

$$C_{11}(u_1) + C_{12}(v_1) + C_{13}(w_1) = 0, \tag{19a}$$

$$C_{21}(u_1) + C_{22}(v_1) + C_{23}(w_1) = 0, \tag{19b}$$

$$C_{31}(u_1) + C_{32}(v_1) + C_{33}(w_1) + PT_{35}(w_1) = 0, \tag{19c}$$

in which coefficients  $C_{ij}(i = 1 \div 3, j = 1 \div 3)$ ,  $T_{35}$  are described in detail in Appendix A.

Equation system (19a,b,c) is used to analyze the state and find the critical mechanical load of the FG CNTRC truncated conical shells.

In this section, an analytical approach is given to investigate the stability of the FG CNTRC truncated conical shells. Assume that a shell is simply supported at both ends. The boundary conditions in this case, are expressed by

$$v_1 = w_1 = 0, M_{x1} = 0 \text{ at } x = x_0, x_0 + L. \tag{20}$$

The approximate solution Eqs. (19) satisfying the boundary conditions (20) may be described as

$$\begin{aligned} u_1 &= X \cos \frac{m\pi(x-x_0)}{L} \sin \frac{n\theta}{2}, \\ v_1 &= Y \sin \frac{m\pi(x-x_0)}{L} \cos \frac{n\theta}{2}, \\ w_1 &= Z \sin \frac{m\pi(x-x_0)}{L} \sin \frac{n\theta}{2}, \end{aligned} \tag{21}$$

where  $m$  is the number of half-waves along a generatrix and  $n$  is the number of full-waves along a parallel circle, and  $X, Y, Z$  are constant coefficients. Due to  $x_0 \leq x \leq x_0 + L; 0 \leq \theta \leq 2\pi$  and for sake of convenience in integration, Eqs. (19a) and (19b) are multiplied by  $x$  and Eq. (19c) by  $x^2$ , and applying Galerkin method for the resulting equations, that are

$$\begin{aligned} \int_{x_0}^{x_0+L} \int_0^{2\pi} \Delta_1 \cos \frac{m\pi(x-x_0)}{L} \sin \frac{n\theta}{2} x \sin \beta d\theta dx &= 0, \\ \int_{x_0}^{x_0+L} \int_0^{2\pi} \Delta_2 \sin \frac{m\pi(x-x_0)}{L} \cos \frac{n\theta}{2} x \sin \beta d\theta dx &= 0, \\ \int_{x_0}^{x_0+L} \int_0^{2\pi} \Delta_3 \sin \frac{m\pi(x-x_0)}{L} \sin \frac{n\theta}{2} x^2 \sin \beta d\theta dx &= 0, \end{aligned} \tag{22}$$

in which

$$\begin{aligned} \Delta_1 &= x[C_{11}(u_1) + C_{12}(v_1) + C_{13}(w_1)], \\ \Delta_2 &= x[C_{21}(u_1) + C_{22}(v_1) + C_{23}(w_1)], \\ \Delta_3 &= x^2[C_{31}(u_1) + C_{32}(v_1) + C_{33}(w_1) + C_{34}N_{x0}(w_1)]. \end{aligned} \tag{23}$$

Substituting expressions (21) and (22) into Eq. (23), after integrating longer and some rearrangements, may be written in the following form

$$d_{11}X + d_{12}Y + d_{13}Z = 0, \tag{24a}$$

$$d_{21}X + d_{22}Y + d_{23}Z = 0, \tag{24b}$$

$$d_{31}X + d_{32}Y + (d_{33} + d_{34}N'_{x0} + d_{35}K_1 + d_{36}K_2)Z = 0, \tag{24c}$$

in which coefficients  $d_{ij}(i = 1 \div 3, j = 1 \div 6)$  are described in detail in Appendix B.

Eq. (24) may be expressed as

$$P = \frac{d_{31}(d_{12}d_{23} - d_{13}d_{22}) + L_{32}(d_{13}d_{21} - d_{11}d_{23}) - d_{33}}{(d_{21}d_{12} - d_{11}d_{22})d_{35}} - \frac{d_{33}}{d_{35}} \tag{25}$$

Eq. (25) gives the buckling mechanical difference for the FG CNTRC truncated conical shells. The minimum value of with respect to  $m$  and  $n$  is called the critical mechanical load.

### 3.2. Thermal buckling

For simplicity, the membrane solution of the equilibrium equations is considered. For this aim, all the moment and rotation terms must be set equal to zero in the equilibrium equations. By solving the membrane form of the equilibrium equations, we find that:

$$\begin{aligned} N_{x0} &= -\frac{x_0 + L}{x} \int_{-h/2}^{h/2} (Q_{11}\alpha_{11} + Q_{12}\alpha_{22})\Delta T dz \\ N_{\theta 0} &= 0 \\ N_{x\theta 0} &= 0 \end{aligned} \tag{26}$$

Consider a conical shell under uniform temperature rise, temperature was increased steadily from the first value to the last value, the difference in temperature  $\Delta T = T_f - T_i$  is a constant.

Take the similar steps of changing as in Section 3.1, we obtain:

$$\Delta T = -\frac{d_{31}(d_{12}d_{23} - d_{22}d_{13}) - d_{32}(d_{11}d_{23} - d_{21}d_{13})}{d_{34}(d_{21}d_{12} - d_{11}d_{22})(L + x_0)P_1} + \frac{d_{33} + d_{33}K_1 + d_{36}K_2}{d_{34}(L + x_0)P_1} \tag{27}$$

in which  $P_1 = \int_{-h/2}^{h/2} (Q_{11}\alpha_{11} + Q_{12}\alpha_{22})\Delta T dz$ .

Eq. (27) gives the buckling temperature difference for the FG CNTRC truncated conical shells under uniform thermal rise. The minimum value of with respect to  $m$  and  $n$  is called the critical temperature.

In case of temperature dependent, the two hand sides of Eq. (27) are temperature dependence which makes it very difficult to solve. Fortunately, we have applied a numerical technique using the iterative algorithm to determine the buckling loads as well as the deflection – load relations in the post-buckling period of the FG CNTRC truncated conical shells. More details, given the material parameter, the geometrical parameter ( $R_1/h, L/R_1$ ) and the value  $\alpha$ , we can use these to determine  $\Delta T$  in (27) as the follows: we choose an initial step for  $\Delta T_1$  on the right hand side in Eq. (27) with  $\Delta T = 0$  (since  $T = T_0 = 300$  K, the initial room temperature). In the next iterative step, we replace the known value of  $\Delta T_1$  found in the previous step to determine the right hand side of Eq. (27)  $\Delta T_2$ . This iterative procedure will stop at the  $k$ th-step if  $\Delta T_k$  satisfies the condition  $|\Delta T - \Delta T_k| \leq \xi$ . Here,  $\Delta T$  is a desired solution for the temperature and  $\xi$  is a tolerance used in the iterative steps.

## 4. Numerical result and discussion

To establish a temperature dependent analysis, a third order

**Table 2**

A comparison on buckling load  $P_{cr}$  (kN) of the FG CNTRC (FG- $\Lambda$ ) conical shells for different semi-vertex angles and length-to-small radius ratios ( $h = 2$  mm,  $R_1/h = 25$ ) with results in Ref. [10].

$V_{cn}^*$	$L/R_1 = 1$	$L/R_1 = 3$					
		$\alpha = 15^\circ$	$\alpha = 30^\circ$	$\alpha = 45^\circ$	$\alpha = 45^\circ$		
0.12	Present	79.62(14,1) <sup>a</sup>	67.92 (1,2)	52.43(18,1)	62.12(1,4)	50.21(1,3)	31.99(10,1)
	Ref. [10]	79.72	69.88	54.67	61.68	48.91	33.40
0.17	Present	120.99(1,3)	108.21(10,1)	83.63(18,1)	103.12(7,1)	83.75(1,2)	53.26(14,1)
	Ref. [10]	123.56	107.10	82.75	102.59	80.85	54.76
0.28	Present	173.11(10,1)	152.16(14,1)	122.14(10,1)	125.39(1,2)	103.03(1,3)	71.09(14,1)
	Ref. [10]	173.25	153.36	121.34	127.76	102.19	70.32

<sup>a</sup> Buckling mode ( $m,n$ ).

**Table 3**

Influences of graded pattern of CNTs on critical buckling mechanical  $P_{cr}$ (MN) of the FG CNTRC conical shells.

$V_{CN}^*$	FG-V CNTRC	FG- $\Lambda$ CNTRC
0.12	481.59 (1,2) <sup>1</sup>	323.91(1,43)
0.17	497.20 (1,3)	485.73 (1,3)
0.28	301.48 (1,4)	279.13 (1,4)

<sup>a</sup> Buckling mode ( $m,n$ ).

interpolation is used to estimate the thermo- mechanical properties of (10,10) armchair SWCNT as a function of temperature. For  $300 \leq T \leq 700$ , variation of thermo- mechanical properties of (10,10) armchair SWCNT with respect to temperature are as shown [22]:

$$\begin{aligned} E_{11}^{CN}(T)[TPa] &= 6.3998 - 4.338417 \times 10^{-3}T + 7.43 \times 10^{-6}T^2 \\ &\quad - 4.458333 \times 10^{-9}T^3 \\ E_{22}^{CN}(T)[TPa] &= 8.02155 - 5.420375 \times 10^{-3}T + 9.275 \times 10^{-6}T^2 \\ &\quad - 5.5625 \times 10^{-9}T^3 \\ G_{12}^{CN}(T)[TPa] &= 1.40755 + 3.476208 \times 10^{-3}T - 6.965 \times 10^{-6}T^2 \\ &\quad + 4.479167 \times 10^{-9}T^3 \\ \alpha_{11}^{CN}(T)[10^{-6}/K] &= -1.12515 + 0.02291688T - 2.887 \times 10^{-5}T^2 \\ &\quad + 1.13625 \times 10^{-8}T^3 \\ \alpha_{22}^{CN}(T)[10^{-6}/K] &= 5.43715 - 0.984625 \times 10^{-4}T + 2.9 \times 10^{-7}T^2 \\ &\quad + 1.25 \times 10^{-11}T^3 \\ E^m &= (3.52 - 0.0034T)GPa \\ \nu^m &= 0.34 \\ \alpha^m &= 45(1 + 0.0005\Delta T)10^{-6}/K \end{aligned}$$

For three different volume fractions of CNTs, these parameters are as:

$$\begin{aligned} \eta_1 &= 0.137, \eta_2 = 1.022 \text{ for } V_{CN}^* = 0.12 \\ \eta_1 &= 0.142, \eta_2 = 1.626 \text{ for } V_{CN}^* = 0.17 \\ \eta_1 &= 0.141, \eta_2 = 1.585 \text{ for } V_{CN}^* = 0.28 \\ \eta_3 &= 0.7\eta_2 \end{aligned}$$

Geometrical characteristics of the shell are

$$\alpha = 30^\circ, R_1/h = 100, L = \sqrt{400R_1h}, h = 0.0127 \text{ m}$$

### 4.1. Comparison studies

Table 2 compares the present result with those of Ref. [10] for FG CNTRC (FG- $\Lambda$ ) conical shells using the first order shear deformation shell theory. The results in the Table 2 compared shows conformity well

**Table 4**  
Influences of graded pattern of CNTs and shell length on critical buckling mechanical  $P_{cr}(MN)$  of FG CNTRC conical shells.

Length	$V_{CN}^*$	FG-V CNTRC	FG-Λ CNTRC
$L = \sqrt{300R_1h}$	0.12	508.77 (23,1)	462.49(20,1)
	0.17	568.75 (19,1)	545.51(18,1)
	0.28	452.83 (14,1)	397.13(12,1)
$L = \sqrt{400R_1h}$	0.12	481.59(1,2)	323.91(1,43)
	0.17	497.20 (1,3)	485.73(1,3)
	0.28	301.48 (1,4)	279.13 (1,4)
$L = \sqrt{500R_1h}$	0.12	271.85 (18,1)	257.91(15,1)
	0.17	340.88 (15,1)	284.64 (13,1)
	0.28	183.56 (10,1)	152.17 (7,1)

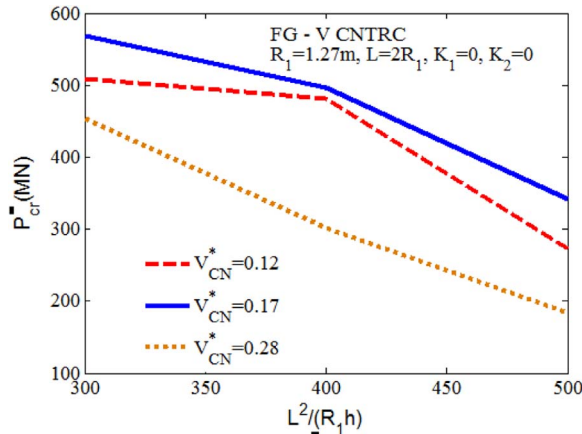


**Fig. 3.** Influences of shell length and volume fraction of fibers on critical buckling mechanical of FG CNTRC conical shells.

**Table 5**  
Influences of graded pattern of CNTs and semi vertex angle  $\alpha$  on critical buckling mechanical  $P_{cr}(MN)$  of FG CNTRC conical shells.

$\alpha$	$V_{CN}^*$	FG-V CNTRC	FG-Λ CNTRC
10°	0.12	553.73 (37,1)	492.75 (33,1)
	0.17	584.34 (31,1)	556.33 (29,1)
	0.28	508.17 (24,1)	429.80 (20,1)
20°	0.12	525.30 (26,1)	485.28 (20,1)
	0.17	544.32 (21,1)	535.60 (20,1)
	0.28	457.35 (16,1)	428.09 (14,1)
30°	0.12	481.59 (1,2)	323.91(1,43)
	0.17	497.20 (1,3)	485.73 (1,3)
	0.28	301.48 (1,4)	279.13 (1,4)
45°	0.12	263.20 (15,1)	237.98 (12,1)
	0.17	322.04 (12,1)	292.26 (11,1)
	0.28	262.40 (9,1)	190.45 (7,1)
60°	0.12	256.58 (15,1)	218.93 (12,1)
	0.17	304.54 (12,1)	266.81 (11,1)
	0.28	202.44 (8,1)	178.08 (7,1)
75°	0.12	132.18 (14,1)	130.57 (12,1)
	0.17	184.95 (12,1)	158.37 (11,1)
	0.28	128.19 (8,1)	104.80 (7,1)

**Table 6**  
Influences of graded pattern of CNTs on critical buckling temperature  $\Delta T_{cr}(K)$  of FG CNTRC conical shells.

$V_{CN}^*$	FG-V CNTRC	FG-Λ CNTRC
0.12	434.0077 (30,2)	405.6702 (29,2)
0.17	473.8662 (30,2)	452.9881 (29,2)
0.28	431.2386 (26,2)	417.6118 (25,2)

**Table 7**  
Influences of graded pattern of CNTs and semi-vertex angle  $\alpha$  on critical buckling temperature  $\Delta T_{cr}(K)$  of FG CNTRC conical shells.

$\alpha$	$V_{CN}^*$	FG-V CNTRC	FG-Λ CNTRC
10°	0.12	504.1794 (33,2)	471.6108 (31,2)
	0.17	512.1293 (32,2)	487.9627 (30,2)
	0.28	490.7945 (29,2)	463.4367 (26,2)
20°	0.12	459.6182 (31,2)	441.5971 (30,2)
	0.17	500.6485 (31,2)	486.2915 (30,2)
	0.28	455.9699 (27,2)	421.8234 (25,2)
30°	0.12	434.0077 (30,2)	405.6702 (29,2)
	0.17	473.8662 (30,2)	452.9881 (29,2)
	0.28	431.2386 (26,2)	390.6118 (25,2)
45°	0.12	408.9583 (29,2)	383.7844 (28,2)
	0.17	416.0395 (28,2)	392.1805 (27,2)
	0.28	404.3764 (25,2)	351.7605 (23,2)
60°	0.12	383.0838 (28,2)	357.094 (27,2)
	0.17	389.0454 (27,2)	363.6357 (26,2)
	0.28	375.8037 (24,2)	350.5158 (23,2)
75°	0.12	357.4137 (27,2)	331.2786 (26,2)
	0.17	362.1960 (26,2)	336.1544 (25,2)
	0.28	347.1808 (23,2)	320.0487 (22,2)

and verify the accuracy of the present method.

4.2. Parametric studies

The effect of graded pattern of CNTs on critical buckling load  $P_{cr}(MN)$  of the FG CNTRC conical shells is shown in Table 3 with geometric parameters of the shells are  $\alpha = 30^\circ$ ,  $R_1/h = 100$ ,  $L = \sqrt{400R_1h}$ ,  $h = 0.0127$  m.

The critical buckling mechanical of conical shells with various graded pattern of fibers and shell length is showed in Table 4 and Fig. 3. In this study, the geometric parameters of the shell is selected as follow:  $R_1/h = 100$ ,  $h = 0.0127$  m and the semi vertex angle of the shell is chosen as  $\alpha = 30^\circ$ . Two different patterns of the CNTs, three different volume fractions of fibers and three different shell lengths are considered. It can be seen that the value of critical mechanical buckling in case of FG-V type of CNTs is larger than that of FG-Λ (Table 3). In addition, at the same pattern of the CNTs, the maximum value of critical buckling mechanical is in the case of  $V_{CN}^* = 0.17$  and the minimum value is in the case of  $V_{CN}^* = 0.28$  (Table 3).

Tables 5–7 and Figs. 4 and 6 shows the influence of various graded pattern of fibers and semi vertex angle  $\alpha$  on critical buckling mechanical (Table 5 and Fig. 4) and critical buckling temperature (Tables 6 and 7 and Fig. 6). In this study, the geometric parameters of the shell is selected as follow:  $R_1/h = 100$ ,  $L = \sqrt{400R_1h}$ ,  $h = 0.0127$  m. Two different patterns of the CNTs, three different volume fractions of fibers and six different semi vertex angles are considered. The semi vertex angles are obtained as an influential parameter on the critical buckling mode, mechanical and temperature of the shell. Increasing the value of the semi vertex angles will make the value of critical buckling mechanical and temperature decrease and vice versa.

Shell length is obtained as an influential parameter on the critical buckling mode and mechanical of the shell. Increasing the value of shell length will make the value of critical buckling mechanical decrease. Analysis the influence of various graded pattern of fibers and shell length on critical buckling temperature, the result gained is the same as above (Table 8 and Fig. 5). This conclusion is similar to the findings of [23,24] for the case of truncated FGM conical shells.

Table 9 shows the influence of various graded pattern of fibers and elastic foundations on critical buckling temperature. In this study, the geometric parameters of the shell is selected as follow:  $R_1/h = 100$ ,  $L = \sqrt{400R_1h}$ ,  $h = 0.0127$  m and the semi vertex angle of the shell is chosen as  $\alpha = 30^\circ$ . Two different patterns of the CNTs, three

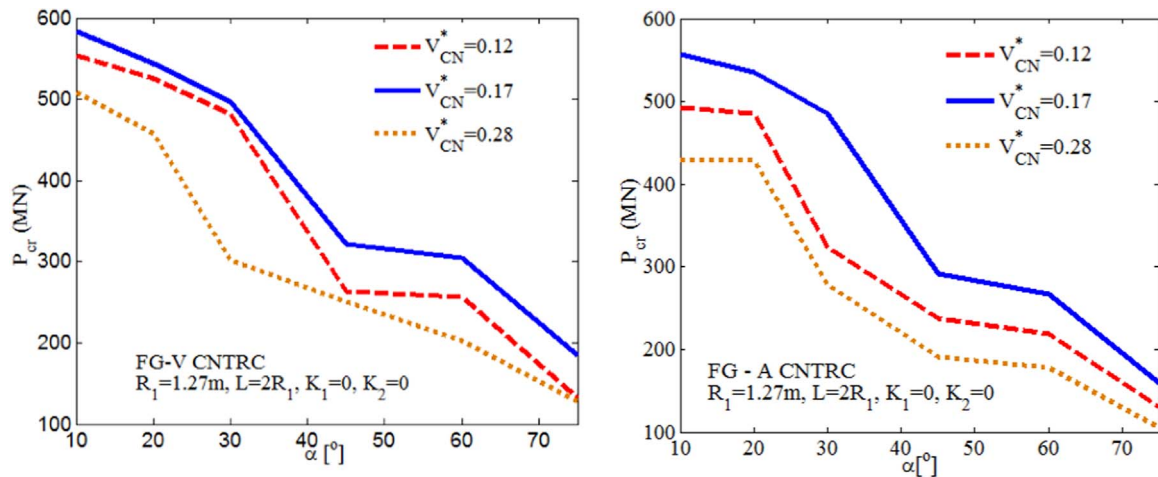


Fig. 4. Influences of semi vertex angle and volume fraction of fibers on critical buckling mechanical of FG CNTRC conical shells.

Table 8

Influences of graded pattern of CNTs and shell length on critical buckling temperature  $\Delta T_{cr}(K)$  of FG CNTRC conical shells.

Length	$V_{CN}^*$	FG-V CNTRC	FG-A CNTRC
$L = \sqrt{300R_1h}$	0.12	469.3857 (27,2)	441.8697 (26,2)
	0.17	511.9253 (27,2)	485.9751 (26,2)
	0.28	449.3161 (23,2)	432.1127 (22,2)
$L = \sqrt{400R_1h}$	0.12	434.0077 (30,2)	405.6702 (29,2)
	0.17	473.8662 (30,2)	452.9881 (29,2)
	0.28	431.2386 (26,2)	417.6118 (25,2)
$L = \sqrt{500R_1h}$	0.12	370.6482 (31,2)	352.6430 (30,2)
	0.17	404.2134 (31,2)	387.8656 (30,2)
	0.28	343.3954 (26,2)	334.7892 (25,2)

different volume fractions of fibers and coefficients ( $K_1, K_2$ ) are considered. The elastic foundations are obtained as an influential parameter on the critical thermal load of the shell. Increasing the value of the elastic foundations will make the value of critical thermal load increase and vice versa. Furthermore, the value of the ground coefficient  $K_2$  affects the critical thermal load  $\Delta T_{cr}$  greater than the ground coefficient  $K_1$ .

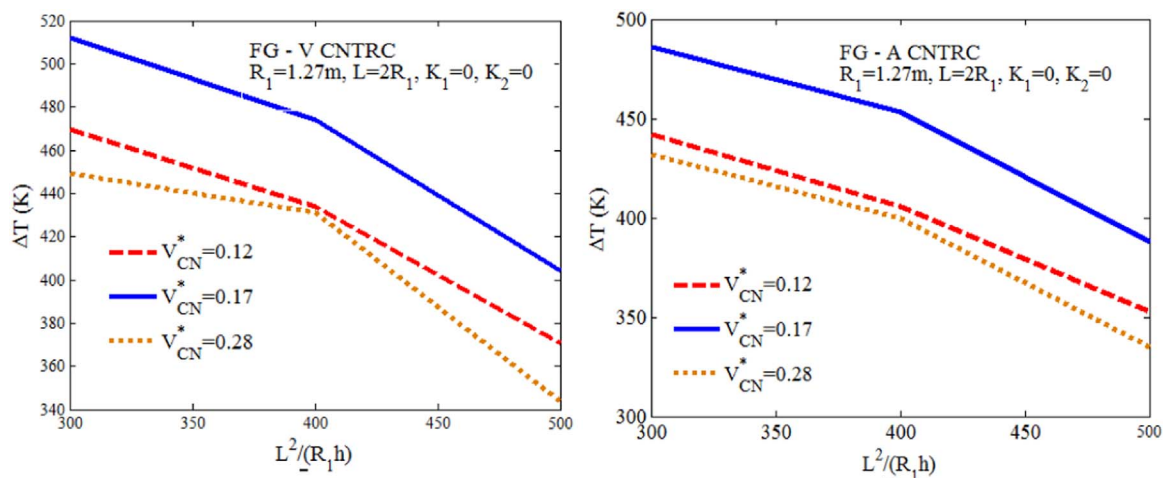


Fig. 5. Influences of shell length and volume fraction of fibers on critical buckling temperature of FG CNTRC conical shells.

### 5. Conclusions

This paper studied the thermal and mechanical stability of functionally graded composite truncated conical shell reinforced by carbon nanotube fibers (the FG CNTRC shell) with temperature-dependent properties in thermal environment and surrounded by the elastic foundations. The following main findings are summarized:

- The buckling mechanical and thermal loads of the FG CNTRC shell are determined.
- The effects of semi-vertex angle, shell length, volume fraction of fibers, distribution pattern of fibers, temperature, elastic foundations on the linear thermal and mechanical buckling loads of the FG CNTRC truncated conical shell in thermal environment. analyzes and discussed:
  - The critical mechanical and thermal load in case of FG-V type of CNTs is larger than that of FG-A.
  - The critical thermal and mechanical loads of FG CNTRC truncated conical shells decrease when the semi-vertex angle  $\alpha$  increases.
  - The critical thermal and mechanical loads of FG CNTRC truncated conical shells decrease when the shell length  $L$  increases.
  - Foundation parameters  $K_1$  and  $K_2$  affect strongly on the critical

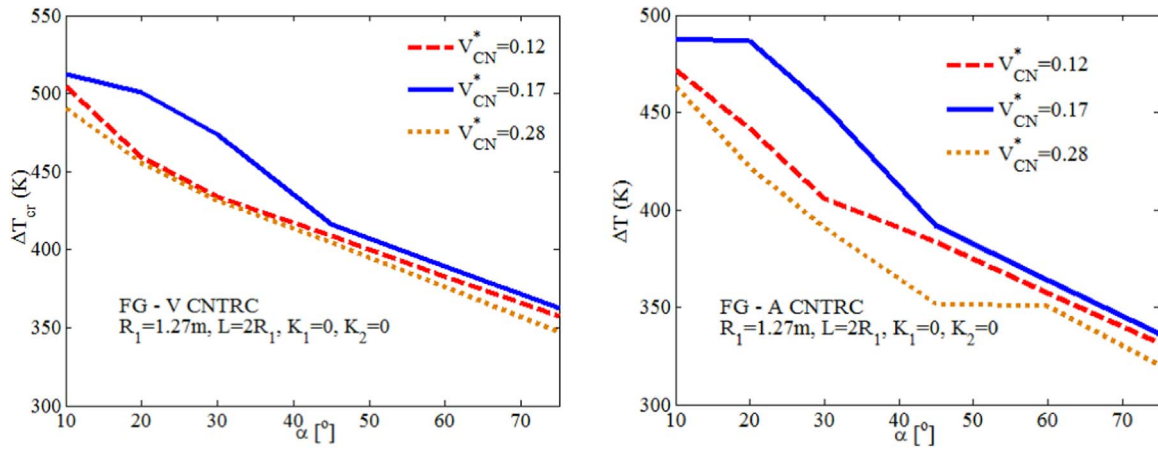


Fig. 6. Influences of semi vertex angle and volume fraction of fibers on critical buckling temperature of FG CNTRC conical shells.

Table 9

Influences of graded pattern of CNTs and elastic foundations on critical buckling temperature  $\Delta T_{cr}$ (K) of FG CNTRC conical shells.

$\Delta T_{cr}$ (K)		$K_1$ (N/m <sup>3</sup> )				
		0	$2 \times 10^7$	$3.5 \times 10^7$	$6 \times 10^7$	
$K_2$ (N/m)	0	$V_{CN}^* = 0.12$	434.0077 (30,2)	495.4154(32,2)	527.3905 (33,2)	560.4634 (34,2)
		$V_{CN}^* = 0.17$	473.8662 (30,2)	506.7667 (31,2)	540.5980 (32,2)	575.5920 (33,2)
		$V_{CN}^* = 0.28$	431.2386 (26,2)	466.3071 (27,2)	502.5686 (28,2)	540.2264 (29,2)
$2 \times 10^5$		$V_{CN}^* = 0.12$	495.4154(32,2)	527.3905 (33,2)	560.4634 (34,2)	660.4634 (34,2)
		$V_{CN}^* = 0.17$	506.7667 (31,2)	540.5980 (32,2)	575.5920 (33,2)	675.5920 (33,2)
		$V_{CN}^* = 0.28$	466.3071 (27,2)	502.5686 (28,2)	540.2264 (29,2)	640.2264 (29,2)
$3.5 \times 10^5$		$V_{CN}^* = 0.12$	527.3905 (33,2)	560.4634 (34,2)	660.4634 (34,2)	760.4634 (34,2)
		$V_{CN}^* = 0.17$	540.5980 (32,2)	575.5920 (33,2)	675.5920 (33,2)	775.5920 (33,2)
		$V_{CN}^* = 0.28$	502.5686 (28,2)	540.2264 (29,2)	640.2264 (29,2)	740.2264 (29,2)

thermal and mechanical loads. Furthermore, the value of the ground coefficient  $K_2$  affects the critical thermal and mechanical loads greater than the ground coefficient  $K_1$ .

**Acknowledgement**

This research is funded by Vietnam National Foundation for Science and Technology Development (NAFOSTED) under grant number 107.02–2015.03. The authors are grateful for this support.

**Appendix A**

$$\begin{aligned}
 C_{11}() &= A_{11}x \frac{\partial^2()}{\partial x^2} + \frac{1}{x \sin^2 \beta} A_{66} \frac{\partial^2()}{\partial \theta^2} + A_{11} \frac{\partial()}{\partial x} - A_{22} \frac{1}{x}(), \\
 C_{12}() &= \frac{1}{\sin \beta} (A_{12} + A_{66}) \frac{\partial^2()}{\partial x \partial \theta} - \frac{1}{x \sin \beta} (A_{22} + A_{66}) \frac{\partial()}{\partial \theta}, \\
 C_{13}() &= -B_{11}x \frac{\partial^3()}{\partial x^3} - \frac{1}{x \sin^2 \beta} (B_{12} + 2B_{66}) \frac{\partial^3()}{\partial x \partial \theta^2} - \frac{1}{x} \cot \beta A_{22}() + \frac{1}{x^2 \sin^2 \beta}(), \\
 C_{21}() &= \frac{1}{\sin \beta} (A_{12} + A_{66}) \frac{\partial^2()}{\partial x \partial \theta} + \frac{1}{x \sin \beta} (A_{22} + A_{66}) \frac{\partial()}{\partial \theta}, \\
 C_{22}() &= \frac{1}{x \sin^2 \beta} A_{22} \frac{\partial^2()}{\partial \theta^2} + x A_{66} \frac{\partial^2()}{\partial x^2} + A_{66} \frac{\partial()}{\partial x} - \frac{1}{x} A_{66}(), \\
 C_{23}() &= -\frac{1}{\sin \beta} (B_{12} + 2B_{66}) \frac{\partial^3()}{\partial x^2 \partial \theta} - \frac{1}{x^2 \sin^3 \beta} B_{22} \frac{\partial^3()}{\partial \theta^3} \\
 &\quad - \frac{1}{x \sin \beta} B_{22} \frac{\partial^2()}{\partial x \partial \theta} + \frac{1}{x \sin \beta} \cot \beta A_{22} \frac{\partial()}{\partial \theta},
 \end{aligned}$$

$$C_{31}() = B_{11}x \frac{\partial^3()}{\partial x^3} + \frac{1}{x \sin^2 \beta} (B_{11} + 2B_{66}) \frac{\partial^3()}{\partial x \partial \theta^2} + 2B_{11} \frac{\partial^2()}{\partial x^2} + \frac{1}{x^2 \sin^2 \beta} B_{22} \frac{\partial^2()}{\partial \theta^2} - \left[ A_{12} \cot \beta + \frac{1}{x} B_{22} \right] \frac{\partial()}{\partial x} + \frac{1}{x^2} B_{22}() - \frac{1}{x} \cot \beta A_{22}(),$$

$$C_{32}() = \frac{1}{\sin \beta} (B_{12} + 2B_{66}) \frac{\partial^3()}{\partial x^2 \partial \theta} + \frac{1}{x^2 \sin^3 \beta} B_{22} \frac{\partial^3()}{\partial \theta^3} - \frac{1}{x \sin \beta} B_{22} \frac{\partial^2()}{\partial x \partial \theta} + \left[ \frac{1}{x^2 \sin \beta} B_{22} - \frac{1}{x \sin \beta} \cot \beta A_{22} \right] \frac{\partial()}{\partial \theta},$$

$$C_{33}() = -D_{11}x \frac{\partial^4()}{\partial x^4} - \frac{1}{x^3 \sin^4 \beta} D_{22} \frac{\partial^4()}{\partial \theta^4} - \frac{2}{x \sin^2 \beta} (D_{12} + 2D_{66}) \frac{\partial^4()}{\partial x^2 \partial \theta^2} + \frac{2}{x^2 \sin^2 \beta} (D_{12} + 2D_{66}) \frac{\partial^3()}{\partial x \partial \theta^2} - 2D_{11} \frac{\partial^3()}{\partial x^3} + \left[ \frac{1}{x} D_{22} + 2B_{12} \cot \beta + xK_2 \right] \frac{\partial^2()}{\partial x^2} + \left[ \frac{2}{x^2 \sin^2 \beta} \cot \beta B_{22} - \frac{2}{x^3 \sin^2 \beta} (D_{12} + 2D_{66} + D_{22}) + \frac{K_2}{x \sin^2 \beta} \right] \frac{\partial^2()}{\partial \theta^2} + K_2 \frac{\partial()}{\partial x} - \frac{1}{x^2} D_{22} \frac{\partial()}{\partial x} + \frac{1}{x^2} \cot \beta B_{22}() - \frac{1}{x} \cot^2 \beta A_{22}() - xK_1(),$$

$$C_{34}() = x \frac{\partial^2()}{\partial x^2}$$

$$T_{35}() = -\frac{1}{\pi \sin 2\alpha} \frac{\partial^2()}{\partial x^2}$$

**Appendix B**

$$d_{11} = -\frac{m^2 \pi^3 (\sin \alpha) A_{11}}{2L^2} \left[ \frac{(x_0 + L)^4 - x_0^4}{4} + \frac{3L^3(2x_0 + L)}{4m^2 \pi^2} \right] + \frac{\pi A_{11} (\sin \alpha) L(2x_0 + L)}{4} - \frac{\pi (\sin \alpha) L(2x_0 + L)}{4} A_{22} - \frac{n^2 \pi A_{66} L(2x_0 + L)}{16 \sin \alpha},$$

$$d_{12} = -\frac{\pi^2 mn (A_{12} + A_{66})}{4L} \left[ \frac{(x_0 + L)^3 - x_0^3}{3} + \frac{L^3}{2m^2 \pi^2} \right] - \frac{nL^2}{8m} (A_{22} + A_{66}),$$

$$d_{13} = \frac{mn^2 \pi^2 (B_{12} + 2B_{66})(2x_0 + L)}{16 \sin \alpha} + \frac{m\pi^2 (\sin \alpha) B_{22}(2x_0 + L)}{4} + \frac{\pi^2 m (\sin \alpha) (\cot \alpha) A_{12}}{L} \left[ \frac{(x_0 + L)^3 - x_0^3}{6} + \frac{L^3}{4m^2 \pi^2} \right] + \frac{\pi^4 m^3 \sin \alpha B_{11}}{2L^3} \left[ \frac{(x_0 + L)^4 - x_0^4}{4} + \frac{3L^3(2x_0 + L)}{4m^2 \pi^2} \right] + \frac{\pi^4 m^3 (\sin \alpha) C_1^0}{2L^3} \left[ \frac{(x_0 + L)^3 - x_0^3}{3} + \frac{L^3}{2m^2 \pi^2} \right] - \frac{\pi^2 m B_{11} (\sin \alpha) (2x_0 + L)}{4}$$

$$\begin{aligned}
 d_{21} &= -\frac{mn\pi^2(A_{12} + A_{66})}{12L}[(x_0 + L)^3 - x_0^3] + \frac{nL^2(A_{12} + A_{66})}{8m} - \frac{nL^2}{8m}(A_{22} + A_{66}), \\
 d_{22} &= -\frac{n^2\pi L(2x_0 + L)}{16\sin\alpha}A_{22} - \frac{\pi A_{66}(\sin\alpha)L(2x_0 + L)}{2} \\
 &\quad - \frac{m^2\pi^3 A_{66}\sin\alpha}{8L^2}[(x_0 + L)^4 - x_0^4] + \frac{3\pi A_{66}(\sin\alpha)L(2x_0 + L)}{8}, \\
 d_{23} &= \frac{n^3\pi LB_{22}}{16\sin^2\alpha} + \frac{m^2n\pi^3(B_{12} + 2B_{66})}{2L^2}\left[\frac{(x_0 + L)^3 - x_0^3}{6} - \frac{L^3}{4m^2\pi^2}\right] \\
 &\quad + \frac{n\pi(\cot\alpha)L(2x_0 + L)}{8}A_{22} + \frac{n\pi LB_{22}}{8}, \\
 d_{31} &= -\frac{m^2\pi^3 B_{11}(\sin\alpha)}{L^2}\left[\frac{L}{2m\pi}(x_0^3 - (x_0 + L)^3) + \frac{3L^4}{4m^3\pi^3}\right] \\
 &\quad + \frac{n^2 B_{22}L^2}{16m\sin\alpha} - \frac{B_{22}(\sin\alpha)L^2}{4m} + \\
 &\quad + A_{22}\frac{L^2(2x_0 + L)\cot\alpha\sin\alpha}{4m} \\
 &\quad + \frac{m^3\pi^4\sin\alpha B_{11}}{L^3}\times\left[\frac{(x_0 + L)^5 - x_0^5}{10} + \frac{L^2(x_0^3 - (x_0 + L)^3)}{2m^2\pi^2} + \frac{3L^5}{4m^4\pi^4}\right] \\
 &\quad + \frac{m^3\pi^4\sin\alpha C_1^0}{L^3}\left[\frac{(x_0 + L)^4 - x_0^4}{8} - \frac{3L^3(2x_0 + L)}{8m^2\pi^2}\right] \\
 &\quad + \frac{mn^2\pi^2(B_{12} + 2B_{66})}{4L\sin\alpha}\left[\frac{(x_0 + L)^3 - x_0^3}{6} - \frac{L^3}{4m^2\pi^2}\right] \\
 &\quad + \frac{m\pi^2 A_{12}\cot\alpha\sin\alpha}{L}\left[\frac{(x_0 + L)^4 - x_0^4}{8} - \frac{3L^3(2x_0 + L)}{8m^2\pi^2}\right] \\
 &\quad + \frac{m\pi^2(\sin\alpha)B_{22}}{L}\left[\frac{(x_0 + L)^3 - x_0^3}{6} - \frac{L^3}{4m^2\pi^2}\right], \\
 d_{32} &= -\frac{\pi m(B_{22})L(2x_0 + L)}{4} + \frac{\pi m^3(B_{22})L(2x_0 + L)}{32\sin^2\alpha} \\
 &\quad + \frac{m^2n\pi^3(B_{12} + 2B_{66})}{2L^2}\left[\frac{(x_0 + L)^4 - x_0^4}{8} - \frac{3L^3(2x_0 + L)}{8m^2\pi^2}\right] \\
 &\quad + \frac{\pi m\cot\alpha}{2}A_{22}\left[\frac{(x_0 + L)^3 - x_0^3}{6} - \frac{L^3}{4m^2\pi^2}\right], \\
 d_{33} &= \frac{\pi n^2 L(D_{12} + 2D_{66})}{8\sin\alpha} + \frac{\pi^4 m^3 D_{11}\sin\alpha}{L^3}\times\left[\frac{L(x_0^3 - (x_0 + L)^3)}{2m\pi} + \frac{3L^4}{4m^3\pi^3}\right] \\
 &\quad + \frac{\pi L\sin\alpha}{4}(D_{22}) + \frac{\pi(B_{22} + C_2)L(2x_0 + L)\cot\alpha\sin\alpha}{4} - \frac{\pi^5 m^4\sin\alpha D_{11}}{L^4} \\
 &\quad \times\left[\frac{(x_0 + L)^5 - x_0^5}{10} + \frac{L^2}{2m^2\pi^2}(x_0^3 - (x_0 + L)^3) + \frac{3L^5}{4m^4\pi^4}\right] \\
 &\quad - \frac{\pi m^4 L}{32\sin^3\alpha}(D_{22}) \\
 &\quad - \frac{\pi^3 m^2 n^2(D_{12} + 2D_{66})}{2L^2\sin\alpha}\left[\frac{(x_0 + L)^3 - x_0^3}{6} - \frac{L^3}{4m^2\pi^2}\right] \\
 &\quad - \frac{\pi^3 m^2\sin\alpha}{L^2}(D_{22})\left[\frac{(x_0 + L)^3 - x_0^3}{6} - \frac{L^3}{4m^2\pi^2}\right] \\
 &\quad + \frac{\pi m^2 L}{4\sin\alpha}(D_{12} + 2D_{66} + D_{22}) \\
 &\quad - \pi\cot^2\alpha\sin\alpha(A_{22})\left[\frac{(x_0 + L)^3 - x_0^3}{6} - \frac{L^3}{4m^2\pi^2}\right] \\
 &\quad - \frac{\pi^3 m^2 B_{12}\cos\alpha}{4L^2}[(x_0 + L)^4 - x_0^4] + \frac{3\pi L}{4}B_{12}\cos\alpha(2x_0 + L) \\
 &\quad - \frac{\pi n^2 B_{22}(\cot\alpha)L(2x_0 + L)}{8\sin\alpha},
 \end{aligned}$$

$$d_{34} = -\frac{m^2 \pi^3 \sin \alpha}{L^2} \left[ \frac{(x_0 + L)^4 - x_0^4}{8} + \frac{3}{8} \frac{L^2}{m^2 \pi^2} (x_0^2 - (x_0 + L)^2) \right],$$

$$d_{35} = -\pi \sin \alpha \left[ \frac{(x_0 + L)^5 - x_0^5}{10} + \frac{L^2 (x_0^3 - (x_0 + L)^3)}{2m^2 \pi^2} + \frac{3L^5}{4m^4 \pi^4} \right],$$

$$d_{36} = \frac{\pi^2 m \sin \alpha}{2L} \left[ \frac{L(x_0^3 - (x_0 + L)^3)}{2m\pi} + \frac{3L^4}{4m^3 \pi^3} \right]$$

$$- \frac{\pi^3 m^2 \sin \alpha}{L^2} \left[ \frac{(x_0 + L)^5 - x_0^5}{10} + \frac{L^2 (x_0^3 - (x_0 + L)^3)}{2m^2 \pi^2} + \frac{3L^5}{4m^4 \pi^4} \right].$$

## References

- [1] K.M. Liew, Z.X. Lei, L.W. Zhang, Mechanical analysis of functionally graded carbon nanotube reinforced composites: a review, *Compos. Struct.* 120 (2015) 90–97.
- [2] M. Koizumi, FGM activities in Japan, *Compos. Part B: Eng.* 28 (1997) 1–4.
- [3] N.D. Duc, *Nonlinear Static and Dynamic Stability of Functionally Graded Plates and Shells*, Vietnam National University Press, Hanoi, 2014.
- [4] H.S. Shen, Nonlinear bending of functionally graded carbon nanotube reinforced composite plates in thermal environments, *Compos. Struct.* 91 (2009) 9–19.
- [5] M.S. Jafari, A.B. Sobhani, V. Khoshkharesh, A. Taherpour, Mechanical buckling of nanocomposite rectangular plate reinforced by aligned and straight single walled carbon nanotubes, *Compos. Part B: Eng.* 43 (2012) 2031–2040.
- [6] Z.X. Lei, L.M. Liew, J.L. Yu, Buckling analysis of functionally graded carbon nanotube-reinforced composite plates using the element-free kp-Ritz method, *Compos. Struct.* 98 (2013) 160–168.
- [7] J.E. Jam, Y. Kiani, Buckling of pressurized functionally graded carbon nanotube reinforced conical shells, *Compos. Struct.* 125 (2015) 586–595.
- [8] S.K. Jalali, M. Heshmati, Buckling analysis of circular sandwich plates with tapered cores and functionally graded carbon nanotubes-reinforced composite face sheets, *Thin-Walled Struct.* 100 (2016) 14–24.
- [9] L.W. Zhang, W.C. Cui, K.M. Liew, Vibration analysis of functionally graded carbon nanotube reinforced composite thick plates with elastically restrained edges, *Int. J. Mech. Sci.* 103 (2015) 9–21.
- [10] R. Ansari, J. Torabi, Numerical study on the buckling and vibration of functionally graded carbon nanotube-reinforced composite conical shells under axial loading, *Compos. Part B-Eng.* 95 (2016) 196–208.
- [11] L.W. Zhang, Z.X. Lei, K.M. Liew, Buckling analysis of FG-CNT reinforced composite thick skew plates using an element-free approach, *Compos. Part B: Eng.* 75 (2015) 36–46.
- [12] H.S. Shen, Postbuckling of nanotube-reinforced composite cylindrical shells in thermal environments, part I: axially-loaded shells, *Compos. Struct.* 93 (2011) 2096–2108.
- [13] H.S. Shen, Postbuckling of nanotube-reinforced composite cylindrical shells in thermal environments, part II: pressure-loaded shells, *Compos. Struct.* 93 (2011) 2496–2503.
- [14] H.S. Shen, Torsional postbuckling of nanotube-reinforced composite cylindrical shells in thermal environments, *Compos. Struct.* 116 (2014) 477–488.
- [15] H.S. Shen, Y. Xiang, Postbuckling of nanotube-reinforced composite cylindrical shells under combined axial and radial mechanical loads in thermal environment, *Compos. Part B: Eng.* 52 (2013) 311–322.
- [16] H.S. Shen, Z.H. Zhu, Buckling and postbuckling behavior of functionally graded nanotube-reinforced composite plates in thermal environments, *CMC-Comput. Mater. Contin.* 18 (2010) 155–182.
- [17] J. Torabi, Y. Kiani, M.R. Eslami, Linear thermal buckling analysis of truncated hybrid FGM conical shells, *Compos. Part B: Eng.* 50 (2013) 265–272.
- [18] M. Akbari, Y. Kiani, M.R. Eslami, Thermal buckling of temperature dependent FGM conical shells with arbitrary edge supports, *Acta Mech.* 226 (2015) 897–915.
- [19] A.H. Sofiyev, Z. Zerín, N. Kuruoglu, Thermoelastic buckling of FGM conical shells under non-linear temperature rise in the framework of the shear deformation theory, *Compos. Part B-Eng.* 108 (2016) 279–290.
- [20] H.S. Shen, C.L. Zhang, Thermal buckling and postbuckling behavior of functionally graded carbon nanotube-reinforced composite plates, *Mater. Des.* 31 (2010) 3403–3411.
- [21] R. Naj, M. Sabzikar Boroujerdy, M.R. Eslami, Thermal and mechanical instability of functionally graded truncated conical shells, *Thin-Walled Struct.* 46 (2008) 65–78.
- [22] M. Mirzaei, Y. Kiani, Thermal buckling of temperature dependent FG-CNT reinforced composite conical shells, *Aerosp. Sci. Technol.* 47 (2015) 42–53.
- [23] N.D. Duc, P.H. Cong, Nonlinear thermal stability of eccentrically stiffened functionally graded truncated conical shells surrounded on elastic foundations, *Eur. J. Mech. – A/Solids* 50 (2015) 120–131.
- [24] N.D. Duc, P.H. Cong, V.M. Anh, V.D. Quang, Tran Phuong, N.D. Tuan, N.H. Thinh, Mechanical and thermal stability of eccentrically stiffened functionally graded conical shell panels resting on elastic foundations and in thermal environment, *J. Compos. Struct.* 132 (2015) 597–609.
- [25] H.S. Shen, Y. Xiang, Postbuckling of axially compressed nanotube-reinforced composite cylindrical panels resting on elastic foundations in thermal environments, *Compos. Part B: Eng.* 67 (2014) 50–61.
- [26] H.S. Shen, Y. Xiang, Nonlinear analysis of nanotube-reinforced composite beams resting on elastic foundations in thermal environments, *Eng. Struct.* 56 (2013) 698–708.
- [27] L.W. Zhang, Z.X. Lei, K.M. Liew, An element-free IMLS-Ritz framework for buckling analysis of FG-CNT reinforced composite thick plates resting on Winkler foundations, *Eng. Anal. Bound. Elem.* 58 (2015) 7–17.
- [28] Z.X. Lei, L.W. Zhang, K.M. Liew, Buckling of FG-CNT reinforced composite thick skew plates resting on Pasternak foundations based on an element-free approach, *Appl. Math. Comput.* 266 (2015) 773–791.
- [29] H.S. Shen, Thermal buckling and postbuckling behavior of functionally graded carbon nanotube-reinforced composite cylindrical shells, *Compos. Part B: Eng.* 43 (2012) 1030–1038.
- [30] H.S. Shen, Y. Xiang, Thermal postbuckling of nanotube-reinforced composite cylindrical panels resting on elastic foundations, *Compos. Struct.* 123 (2015) 383–392.
- [31] N.D. Duc, *Nonlinear Static and Dynamic Stability of Functionally Graded Plates and Shells*, Vietnam National University Press, Hanoi, 2014.
- [32] D.D. Brush, B.O. Almroth, *Buckling of Bars Plates and Shells*, McGraw-Hill, New York, 1975.